

## 3D Numerical Study on Laminar Forced Convection in V-Baffled Square Channel

<sup>1</sup>Amnart Boonloi and <sup>2</sup>Withada Jedsadaratanachai

<sup>1</sup>Department of Mechanical Engineering Technology, College of Industrial Technology, King Mongkut's University of Technology North Bangkok, Bangkok 10800, Thailand

<sup>2</sup>Department of Mechanical Engineering, Faculty of Engineering, King Mongkut's Institute of Technology Ladkrabang, Bangkok 10520, Thailand

Received 2013-02-09, Revised 2013-02-09; Accepted 2013-09-03

### ABSTRACT

The article presents a mathematical study of fully developed periodic laminar flow visualization and heat transfer characteristics in an isothermal wall square-channel fitted with V-shaped baffles on one wall. The computations based on the finite volume method together with the SIMPLE algorithm have been performed. The investigation covers a range of Re based on the hydraulic diameter of the channel,  $Re = 100-1200$ . To create a pair of main streamwise vortex flows through the tested section, the V-baffles with the attack angle of  $30^\circ$  with the main flow direction are mounted in tandem and pointing downstream on the lower channel wall only. Effects of different baffle heights and pitches on heat transfer and pressure drop in the channel are examined and the results obtained are compared with smooth channel with no baffle. The numerical result shows that the presence of the V-baffle yields a significant heat transfer enhancement compared with the smooth channel. It is visible that the main vortex flows, a pair of streamwise twisted vortex (P-vortex) can induce impingement flows on the walls leading to a drastic increase in heat transfer rate over the channel. In addition, the increase in the baffle height leads to the rise in the heat transfer and pressure loss while that in the baffle pitch provides the opposite trend. The predicted results expose that the maximum thermal enhancement factors for the V-baffles with  $BR = 0.3, 0.3$  and  $0.4$ ; and  $PR = 1, 1.5$  and  $2$  are, respectively, about 2.44, 2.29 and 2.37 at higher Re.

**Keywords:** Periodic Flow, Square Channel, Laminar Flow, Heat Transfer, V-Shaped Baffle

### 1. INTRODUCTION

The use of ribs/baffles (Promvongse *et al.*, 2012a; 2012b; Sriromreun *et al.*, 2012) in duct or channel heat exchanger is one of the commonly used passive heat transfer enhancement strategies in single-phase internal flows. Repeatedly positioned ribs/baffles in the channels periodically can interrupt hydrodynamic and thermal boundary layers resulting in a greater increase of the heat transfer rate.

Many investigators had been studied on V-shaped turbulators or vortex generators. Peng *et al.* (2011)

investigated on both experimentally and numerically for convection heat transfer in channels with different types of ribs. The results indicated that the  $45^\circ$  V-shaped continuous ribs have the highest thermal performance. Karwa and Chitoshiya (2013) experimentally studied of thermo-hydraulic performance of a solar air heater with  $60^\circ$  V-down discrete rib roughness on the air flow side of the absorber plate. They found that the enhancement in the thermal efficiency due to the roughness on the absorber plate is found to be 12.5-20% depending on the air flow rate. In addition, influences of angled

**Corresponding Author:** Amnart Boonloi, Department of Mechanical Engineering Technology, College of Industrial Technology, King Mongkut's University of Technology North Bangkok, Bangkok 10800, Thailand

baffles (or thin ribs) placed on two opposite walls of a square channel on heat transfer and flow characteristics were examined numerically (Promvonge and Kwankaomeng, 2010; Promvonge *et al.*, 2010a; 2010b). The investigations revealed that the streamwise vortex flows caused by the angled baffles exist and assist to induce impingement jets on the channel walls leading to a drastic increase in the heat transfer rate.

Although numerous studies on rib and baffle roughened surfaces have been reported in the literature, there has rarely been published on how the fluid flow and heat transfer behavior in the V-baffled channels are influenced by the spacing and height of the baffles, especially for numerical works. Experimental measurements are often limited by the confined space and measurement points available. Therefore, the main aim of the present study is to investigate the fluid flow and heat transfer characteristics in the square channel with different baffle height and spacing intensities using a computer simulation. The numerical computations for three dimensional laminar periodic channel flows over a 30° V-downstream baffle mounted only on the lower square channel wall are conducted.

## 2. MATERIALS AND METHODS

### 2.1. Geometry of Baffled Channel and Arrangement

Figure 1 shows the V-shaped baffles placed repeatedly on the lower wall of a square channel including the computational domain of a periodic flow module employed in the present work. The V-baffles are arranged by letting the V-tip point to downstream flow (V-downstream baffle). The flow under consideration is expected to attain a periodic flow condition in which the velocity field and thermal profile repeat itself from one module to another. The concept of periodically fully developed flow and its solution procedure has been described by (Promvonge *et al.*, 2012b). In the channel module, the air enters at an inlet temperature,  $T_{in}$  and flows over a baffle where  $b$  is the baffle height,  $H$  set to 0.05 m, is the channel height and  $b/H$  is known as the blockage ratio, BR. The distance between the baffles is set to  $L$  in which  $L/H$  is defined as the pitch ratio, PR. To investigate an interaction effect of the baffles with an attack angle,  $\alpha = 30^\circ$  with the flow direction, BR and PR values are varied in a range of BR = 0.1-0.5 and PR = 1.0-2.0 in the present study.

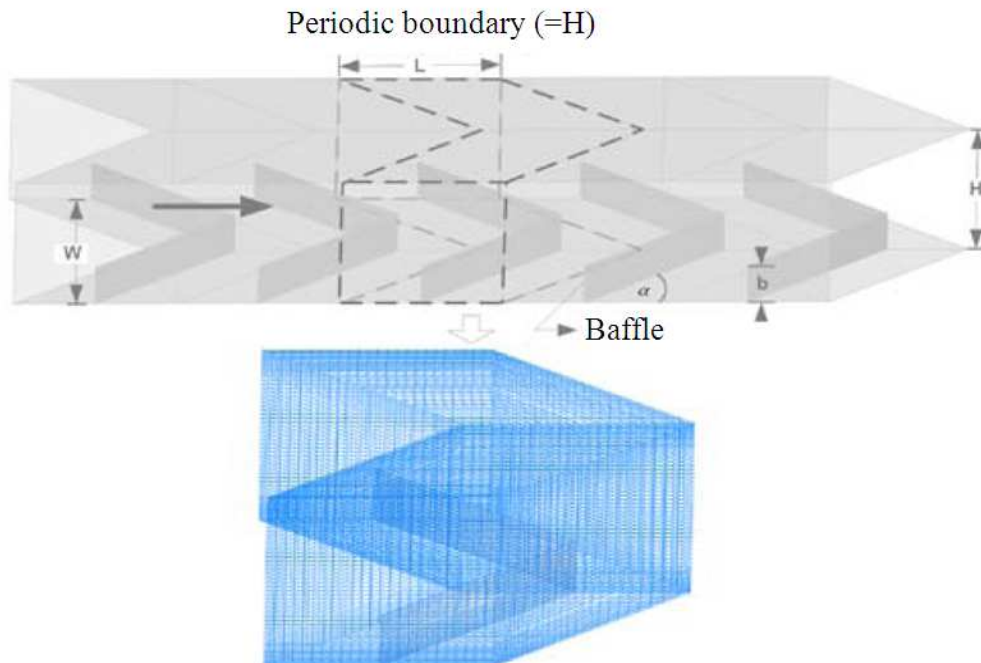


Fig. 1. Channel geometry and computational domain of periodic flow for V-shaped baffle

## 2.2. Mathematical Modeling

Promvonge and Kwankaomen (2010) and Promvonge *et al.* (2010a; 2010b; 2012b), the numerical model for fluid flow and heat transfer in a channel is developed under the following assumptions:

- Three-dimensional, steady, laminar and incompressible air flow
- The flow and heat transfer in the channel is fully developed periodic
- Constant air properties
- Body forces and viscous dissipation are ignored
- Negligible radiation heat transfer

The present problem is three-dimensional, laminar and steady. The relevant equations are the Navier–Stokes equations and energy equation. The equations in the tensor notation form are as follows.

Continuity Equation 1:

$$\frac{\partial}{\partial x_i}(\rho u_i) = 0 \tag{1}$$

Momentum Equation 2:

$$\frac{\partial(\rho u_i u_j)}{\partial x_j} = -\frac{\partial p}{\partial x_i} + \frac{\partial}{\partial x_j} \left[ \mu \left( \frac{\partial u_i}{\partial x_j} + \frac{\partial u_j}{\partial x_i} \right) \right] \tag{2}$$

Energy Equation 3:

$$\frac{\partial}{\partial x_i}(\rho u_i T) = \frac{\partial}{\partial x_j} \left( \Gamma \frac{\partial T}{\partial x_j} \right) \tag{3}$$

where,  $\Gamma$  is the thermal diffusivity and is given by Equation 4:

$$\Gamma = \frac{\mu}{Pr} \tag{4}$$

Apart from the energy equation discretized by the QUICK scheme, the governing equations were discretized by the power law scheme, decoupling with the SIMPLE algorithm and solved using a finite volume approach (Versteeg and Malalasekera, 2007). The solutions were considered to be converged when the normalized residual values were less than  $10^{-6}$  for all variables except for the energy equation set to be converged at less than  $10^{-9}$ .

Four parameters of interest in the present work are the Reynolds number, friction factor, Nusselt number and thermal enhancement factor (Promvonge *et al.*, 2012b).

## 2.3. Boundary Conditions

Promvonge and Kwankaomen (2010) and Promvonge *et al.* (2010a; 2010b; 2012b), periodic boundaries are used for the inlet and outlet of the flow domain. The constant mass flow rate of air with 300 K is assumed in the flow direction rather than constant pressure drop due to periodic flow and thermal profile conditions. The inlet and outlet profiles for the velocities and heat transfer must be identical. The physical properties of the air have been assumed to remain constant at average bulk temperature. Impermeable boundary and no-slip wall conditions have been implemented over the channel walls as well as the baffle. The constant temperature of all channel walls is maintained at 310 K while the V-baffle is set to an adiabatic wall condition.

## 3. RESULTS AND DISCUSSION

### 3.1. Accuracy Validation and Grid system

For validating the accuracy of numerical solutions, the computations of fully developed laminar forced convection in a square channel with no baffle have been carried out to compare with the exact solutions as shown in **Fig. 2a and b**, respectively. The present numerical smooth channel result is found to be in excellent agreement with the exact solutions obtained from the open literature (Incropera *et al.*, 2007) for both the Nusselt number and the friction factor, less than  $\pm 0.5\%$  deviation.

Grid independent tests have been performed by using three different grid systems with 85,600, 125,500 and 245,600 cells to calculate the flow and thermal fields in the baffled channel. The test was conducted for the baffled channel with BR = 0.30, PR = 1 and Re = 800. It is found that the difference in heat transfer and friction coefficients among the grids used is less than 1.3%. Accordingly, the grid system of 85,600 cells is employed to perform the current calculations.

### 3.2. Flow Structure

The flow and vortex coherent structure in a square channel fitted with V-shaped baffles on the lower wall only can be displayed by considering the streamline planes as depicted in **Fig. 3**. Here the streamline planes of the V-baffle modules by connecting the computed modules in series as shown in **Fig. 3a, b and c** are presented at Re = 1000 and BR = 0.3 for (a) PR = 1, (b) PR = 1.5 and (c) PR = 2, respectively.

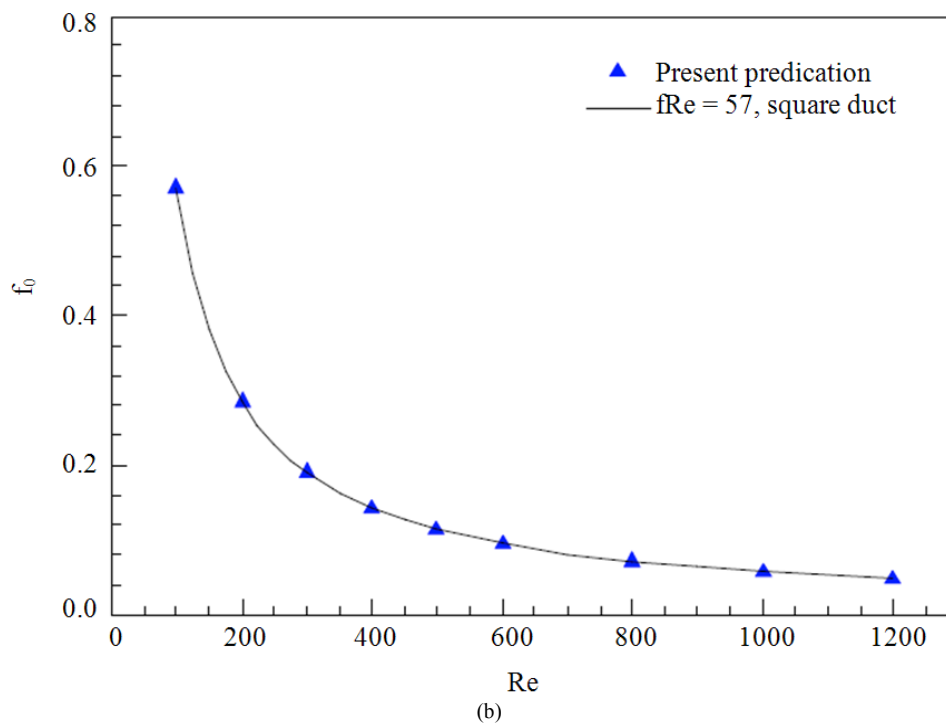
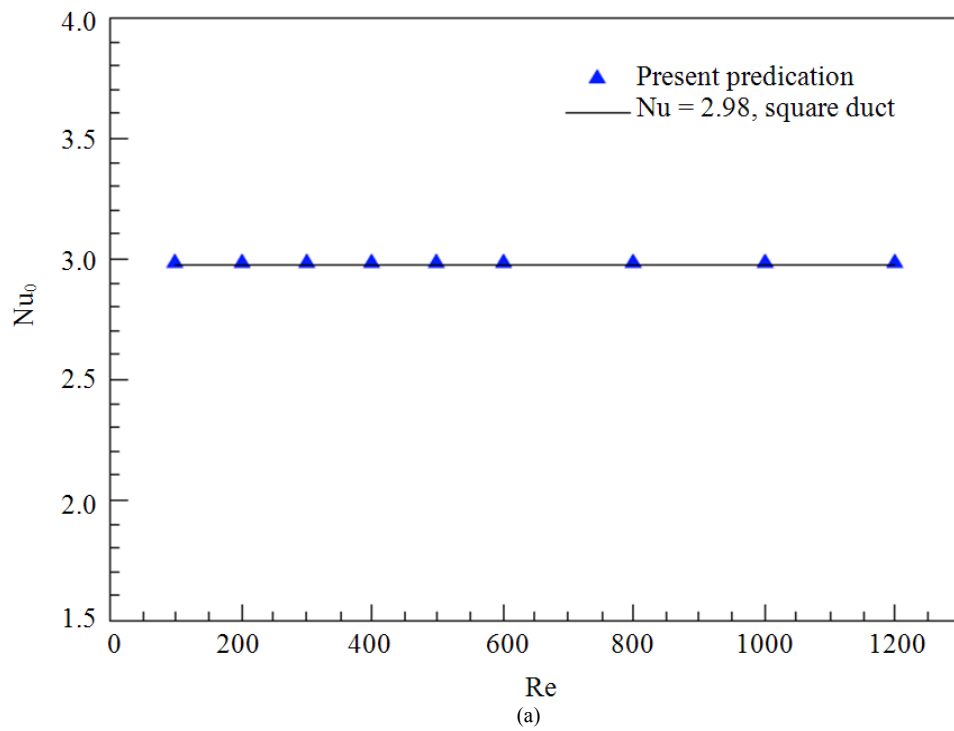
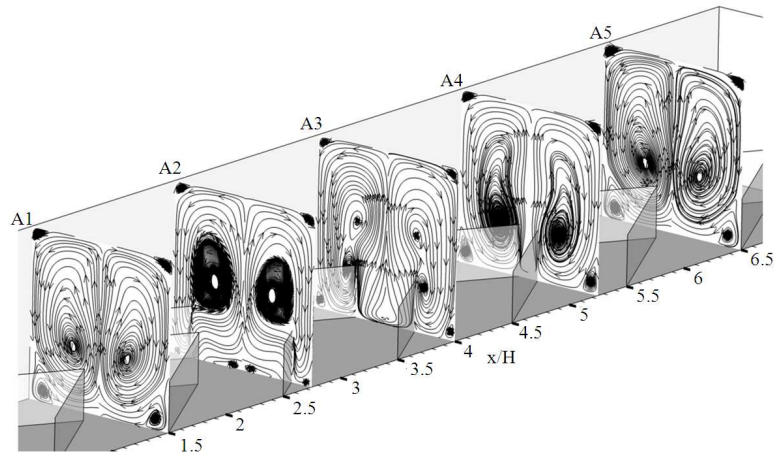
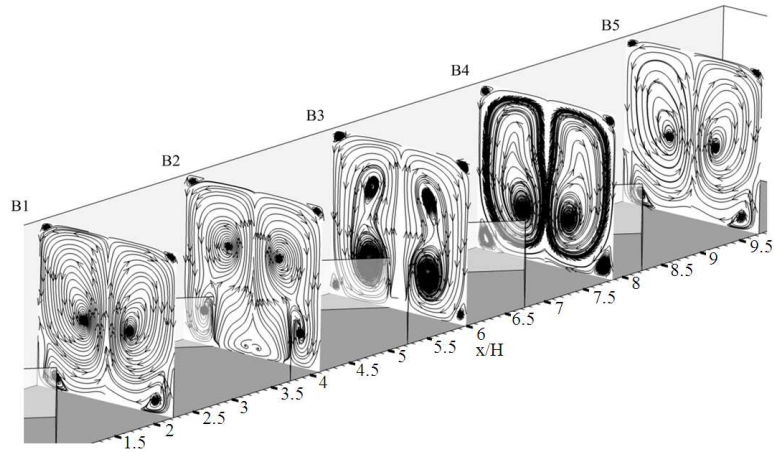


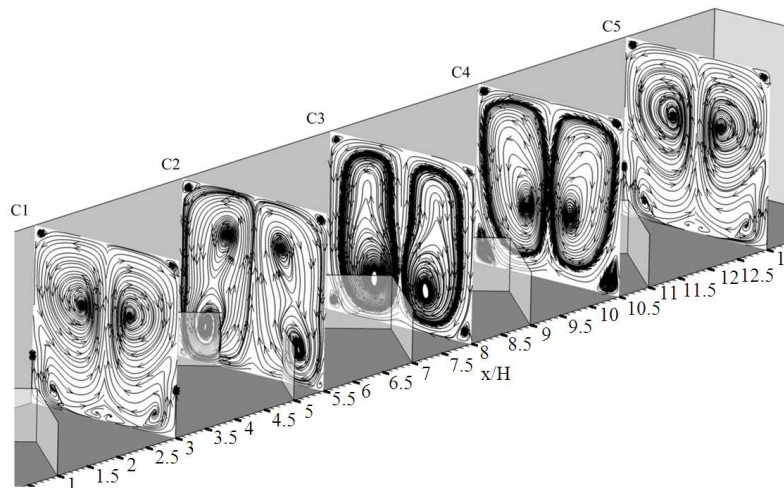
Fig. 2. Validation of (a) Nusselt number and (b) friction factor for smooth channel



(a)



(b)



(c)

**Fig. 3.** Streamlines in transverse planes for (a)  $PR = 1$ , (b)  $PR = 1.5$  and (c)  $PR = 2$  at  $Re = 1000$  and  $BR = 0.3$

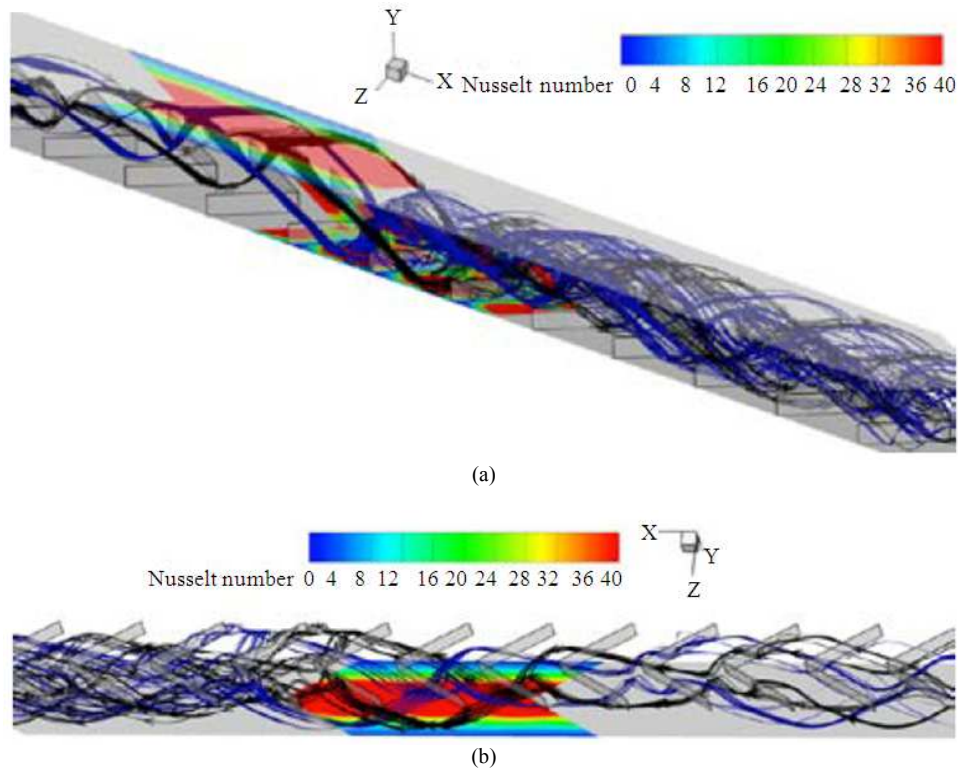


**Fig. 4.** Streamlines of impinging jet of cells on (a) lower and (b) upper walls at  $Re = 1000$ ,  $PR = 1$  and  $BR = 0.3$

It is visible in **Fig. 3** that there are two main vortices flows (or vortex core) in the V-baffled channel, four small vortices at the channel corners. A single module considered herein begins at the Baffle Leading Edge (BLE) to the BLE of the next module. By considering two counter-rotating vortices of the module with  $PR = 1$ , before the fluid flow passes the baffle, two centers of the main counter-rotating vortex flows (common-vortex flow-up) at the BLE plane, plane A1 in **Fig. 3a**, are near the central area at about the baffle tip level while two small vortices appear in the lower corners. When moving to the quarter module pitch location, plane A2, two vortex centers appearing up-stream of the baffle spirally moves up to the central region of the channel. The two small lower corner vortices move close together to the middle area of the lower wall while two new small vortices appear at the lower corners downstream of the baffle. The two upstream main vortex cores seem to be vanishing while two downstream ones including the two small corner vortices are appearing at the half module pitch location as can be seen in plane A3. At the three-quarter pitch location, plane A4, both the two upstream small and main vortex centers completely vanish while the two downstream small and main ones become larger

and make a helical move closer together until passing the baffle V-apex. The two vortex core centers repeat itself when getting to the BLE of the next downstream module, plane A5. This vortex flow pattern is also similar to the cases of  $PR = 1.5$ , planes B1-B5 in **Fig. 3b** and of  $PR = 2$ , planes C1-C5 in **Fig. 3c**, except for the two vortex core centers appearing at different locations.

The plots of streamlines and channel wall heat fluxes showing the impingement jets on the lower and upper walls of the modules at  $PR = 1$ ,  $BR = 0.3$  and  $Re = 1000$  for the V-baffled channel by connecting several modules in the series are portrayed in **Fig. 4a and b**, respectively. In the figure, it can be observed that impinging jets occur repeatedly in a lower wall region of the inter-baffle cavity and in a large region on the upper wall. A close examination reveals that two helical vortex flows from both sides move along the baffle cavity to come close together at the V-tip area before rolling up to impinge on the upper wall and then move across 3-5 modules to impinge again on the lower wall of the modules downstream, depending on  $Re$ ,  $PR$  and  $BR$  values. After impingement, the jet splits over the wall and recombines to become two helical streams (P-vortex) at the nearby baffles:

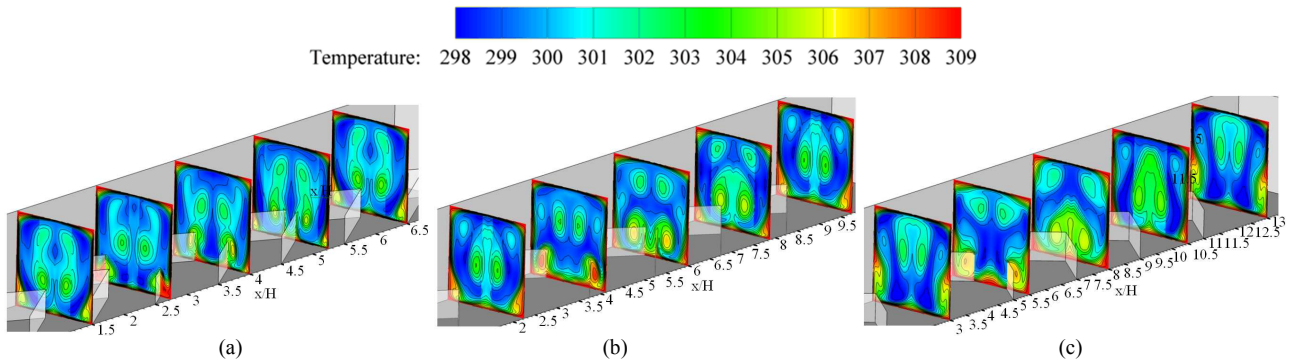


**Fig. 5.** Temperature contours in transverse planes for (a) PR=1, (b) PR = 1.5 and (c) PR = 2, at Re = 1000 and BR = 0.3

One stream joining at the upstream baffle and the other joining at the downstream baffle to create vortex filaments again with shorter pitch lengths. The helical pitch length of the main vortex flow is about 3H-5H before impingement and becomes shorter after impingement.

This means that the two helical vortex flows move along the baffle cavity and rolling up near the V-apex area to pass over three to five baffle modules into the sidewall area before curling down to move along the baffle cavity again to complete the helical flow. If the helical vortex flow strength is sufficiently strong after 3 to 5 helixes, the helical flow becomes impingement flow.

### 3.3. Temperature Field

**Figure 5a, b and c** displays the contour plots of temperature field in transverse planes for the BR = 0.3 V-baffle with (a) PR = 1, (b) PR = 1.5 and (c) PR = 2 at Re = 1000, respectively. In the figure, it is visible that there is a major change in the temperature field throughout the baffled channel. This indicates that the P-vortex flow provides a significant influence on the temperature field. **Fig. 5a, b and c** displays the contour plots of temperature field in transverse planes for the BR = 0.3 V-baffle with (a) PR = 1, (b) PR = 1.5 and (c) PR = 2 at Re = 1000, respectively. In the figure, it is visible that there is a major change in the temperature field throughout the baffled channel. This indicates that the P-vortex flow provides a significant influence on the temperature field, because it can induce better fluid mixing by transporting fluid from the central core to the near wall regions, leading to a high temperature gradient over the heated channel wall. The higher temperature gradient can be observed where the flow impinges the channel walls while the lower one is seen at the corner region and at the area behind the baffle where the

temperature in those regions is somewhat high indicating that low temperature gradient occurs. However, the temperature fields for all the three cases are seen to be similar and almost distributed uniformly in the entire flow indicating excellent mixing of the fluid flow.

### 3.4. Local and Average Nusselt Number

Local  $Nu_x$  contours for the 30° V-shaped baffles with (a) PR = 1, (b) PR = 1.5 and (c) PR = 2 at Re = 1000, BR = 0.3 are shown in **Fig. 6a, b and c**, respectively. In the figure, it is apparent that the higher  $Nu_x$  values over the walls are seen to be in a larger area, especially in the central area of the upper wall. The lower  $Nu_x$  can be observed at the corner regions and the area around the baffle. The peak values are found at the impingement areas on the upper wall and on the inter-baffle cavity. The peak  $Nu_x$  values for the V-baffle are found to be about 14.5 times higher than those for the smooth channel. This indicates a merit of employing the V-baffle over the smooth square channel for enhancing heat transfer.

The variation of the average  $Nu/Nu_0$  ratio with Re values for the V-baffles at various PRs and BRs is depicted in **Fig. 7**. In the figure, it is noted that the  $Nu/Nu_0$  value tends to increase with the rise of BR and Re values while shows an opposite trend with the increase in PR. The maximum  $Nu/Nu_0$  values for PR=1, 1.5 and 2 are around 14.49, 14.40 and 13.63 at BR = 0.5, Re = 1200, respectively. The scrutiny of **Fig. 7** reveals that the V-baffle yields the heat transfer rate of about 1.00-14.49 times over the channel with no baffle, depending on the BR, PR and Re values.

### 3.5. Pressure loss

The variation of the friction factor ratio,  $f/f_0$  with Re values at various BRs and PRs is displayed in **Fig. 8**.

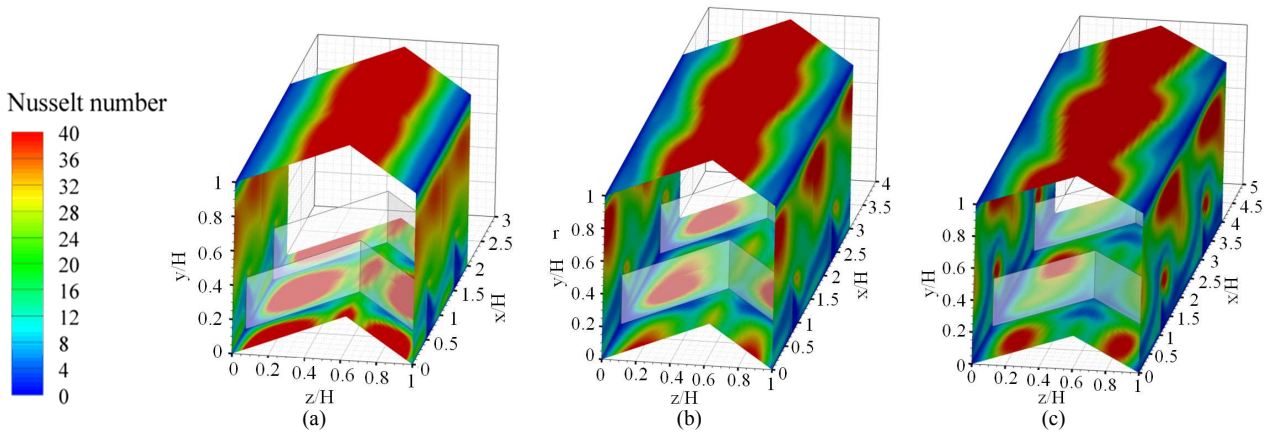


Fig. 6.  $Nu_x$  Contours for (a) PR = 1, (b) PR = 1.5 and (c) PR = 2 at Re = 1000 and BR = 0.3

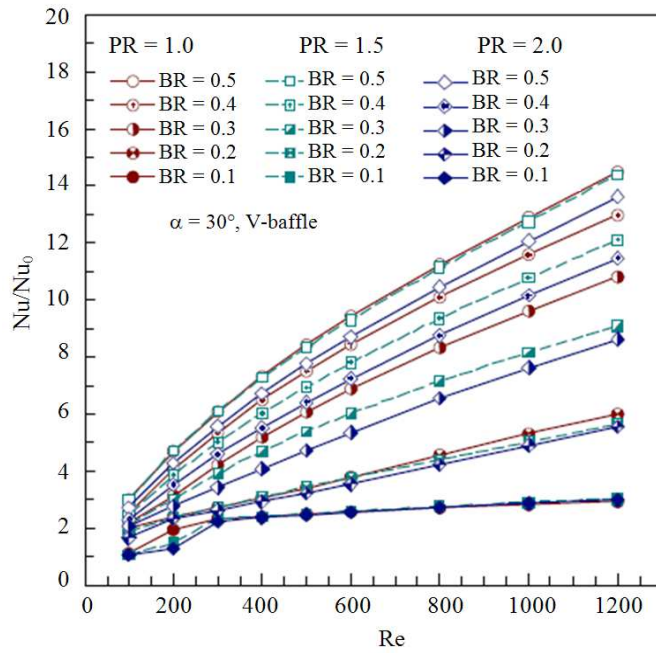


Fig. 7. Variation of  $Nu/Nu_0$  with Reynolds number for various BRs and PRs

In the figure, it is obvious that the  $f/f_0$  value tends to increase with the increment of Re and BR values but to decrease with increasing PR values. The PR=1 baffle case provides the highest  $f/f_0$  value while the PR = 2 baffle yields the lowest for similar BRs. The friction factor for the V-baffles appear to be about 2.2-313.3 times higher than that for the channel with no baffle. Thus the flow blockage due to the presence of the baffles is a vital factor to cause a high pressure drop. Effect of PR values on the  $f/f_0$  value is also

depicted in Fig. 8. It is worth noting that the use of higher PR value leads to a considerable reduction of friction factor.

### 3.6. Performance Evaluation

Figure 9 shows the variation of Thermal Enhancement Factor (TEF) for air flowing in the V-baffled square channel. In the figure, the TEF of the V-baffle tends to increase with the rise of Re and BR values whereas shows a uniform trend for BR = 0.1 at Re > 300.

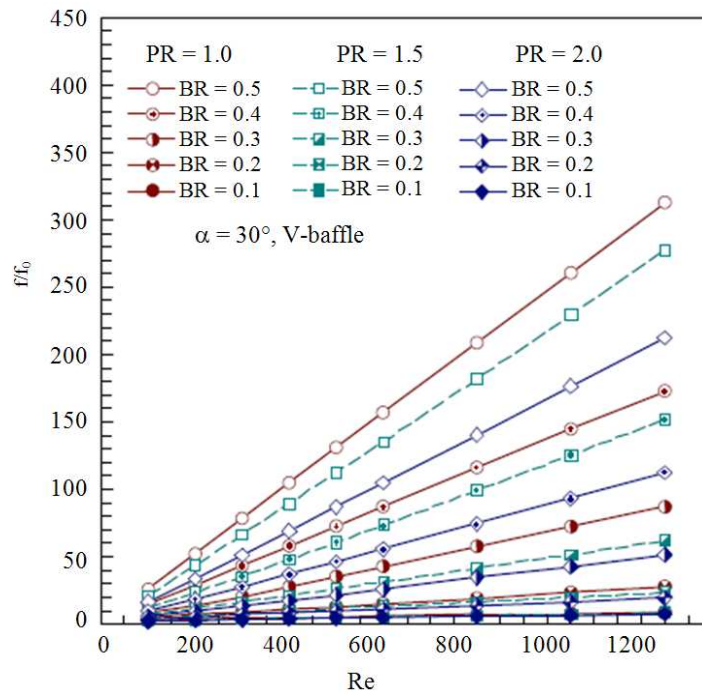


Fig. 8. Variation of  $f/f_0$  with Reynolds number at various BRs and PRs

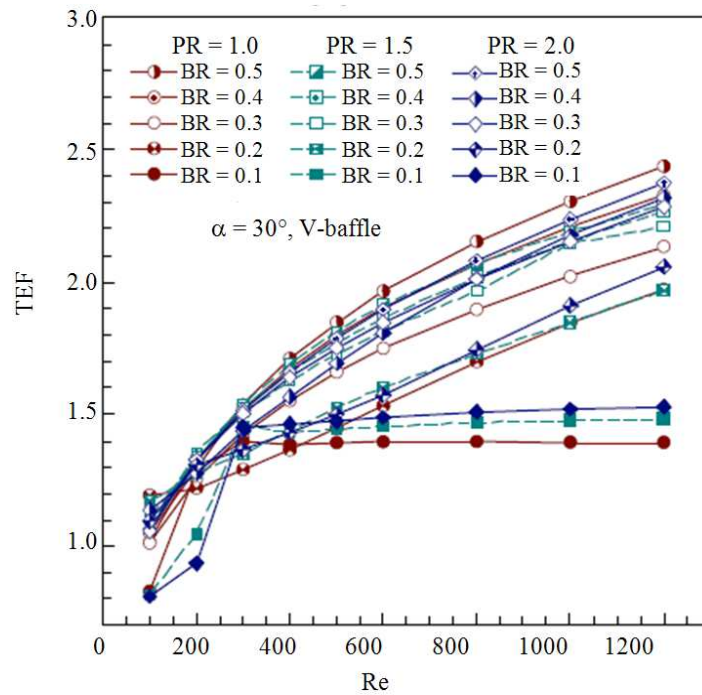
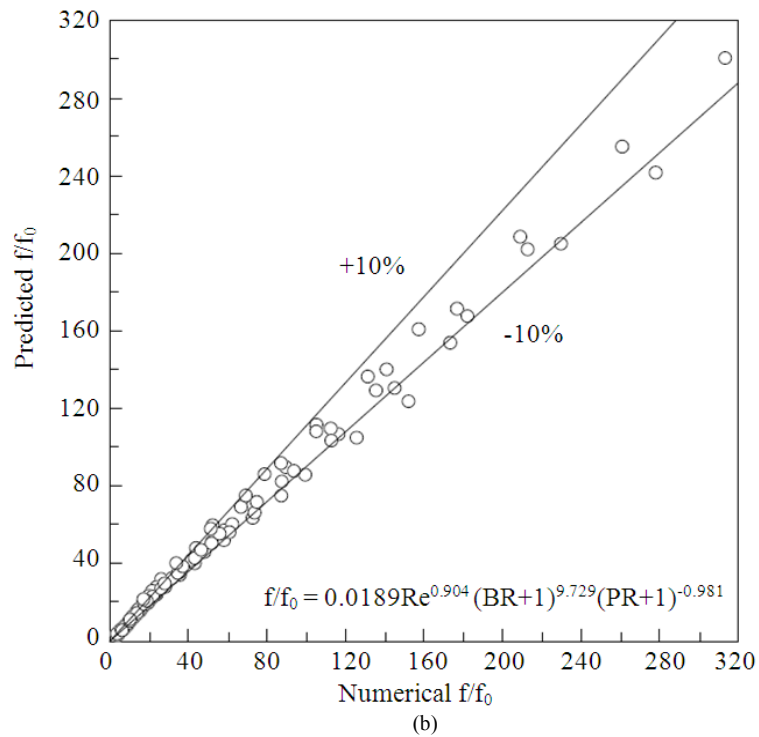
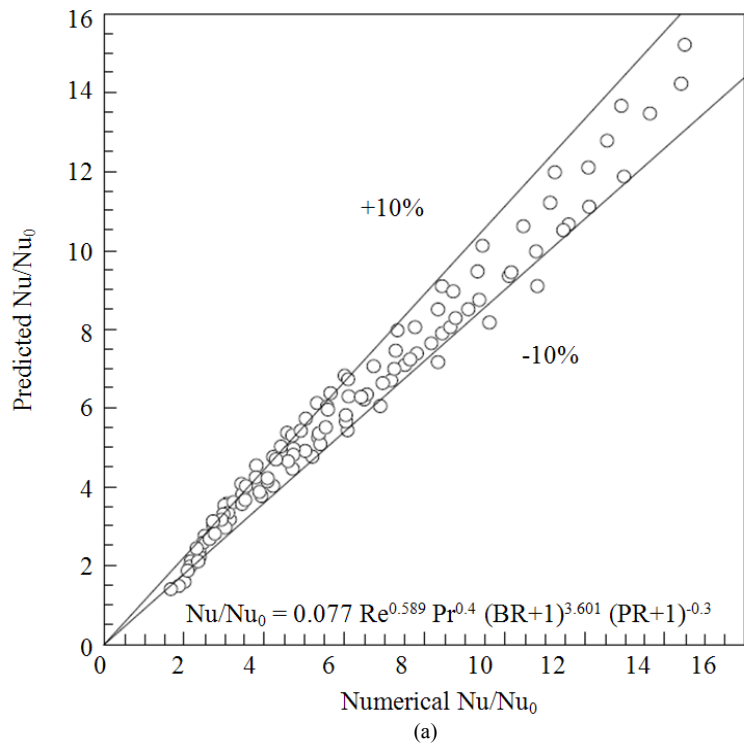


Fig. 9. Comparison of TEF at various BRs and PRs



**Fig. 10.** Comparison of (a)  $Nu/Nu_0$  and (b)  $f/f_0$  obtained from the present correlations with numerical data

The highest TEF for the V-baffle with PR = 1 and 1.5 is found at BR = 0.3 while that with PR = 2 is at BR = 0.4. The TEF values of all the V-baffle cases are seen to be above unity except for BR = 0.1,  $Re \leq 200$  and vary between 0.80 and 2.44, depending on the BR, PR and Re values. It is interesting to note that at  $Re = 1200$ , the maximum TEF values for the V-baffle with PR = 1, 2 and 1.5 are, respectively, 2.44, 2.37 and 2.29 at BR = 0.3, 0.4 and 0.3.

The Nusselt number and friction factor values obtained from using the 30° V-baffle are correlated as below:

$$Nu / Nu_0 = 0.077 Re^{0.579} Pr^{0.4} (BR + 1)^{3.601} (PR + 1)^{-0.3} \quad (5)$$

$$f / f_0 = 0.0189 Re^{-0.904} (BR + 1)^{9.729} (PR + 1)^{-0.981} \quad (6)$$

Comparisons of the  $Nu/Nu_0$  and the  $f/f_0$  obtained from the present prediction with those from the above correlations, Equation 10 and 11 are depicted in **Fig. 10a and b**, respectively. In the figure, the majority of the predicted data falls within  $\pm 10\%$  for the present correlations for both  $Nu/Nu_0$  and  $f/f_0$ .

#### 4. CONCLUSION

Numerical computations of laminar periodic flow and heat transfer characteristics in a square channel fitted with 30° V-baffle elements in tandem on the lower wall only are performed. The P-vortex flow created by the V-baffle exists and helps to induce impingement flows over the channel walls leading to a drastic increase in heat transfer in the channel. The order of heat transfer enhancement is about 1.00-14.49 times for using the V-baffle with BR = 0.1-0.5 and PR = 1, 1.5 and 2. However, the heat transfer augmentation is associated with enlarged pressure loss ranging from 2.18 to 313.24 times above the smooth channel depending on the BR, PR and Re values. It is found that the optimum TEF value in the present investigation is about 2.44 for V-baffle with BR = 0.3, PR = 1 at  $Re = 1200$ .

#### 5. ACKNOWLEDGEMENT

This research was funded by College of Industrial Technology, King Mongkut's University of Technology North Bangkok, Thailand.

The author would like to thank Assoc.Prof.Dr Pongjet Promvong and Dr. Withada Jedsadaratanachai, KMITL for suggestions.

#### 6. REFERENCES

- Incropera, F., P.D. Dewitt, T.L. Bergman and A.S. Lavine, 2007. Introduction to Heat Transfer. 6th Edn., John Wiley and Sons Inc., ISBN-10: 0471794716.
- Karwa, R. and G. Chitoshiya, 2013. Performance study of solar air heater having v-down discrete ribs on absorber plate. Energy, 55: 939-955. DOI: 10.1016/j.energy.2013.03.068
- Peng, W., P.X. Jiang, Y.P. Wang and B.Y. Wei, 2011. Experimental and numerical investigation of convection heat transfer in channels with different types of ribs. Applied Thermal Eng., 31: 2702-2708. DOI: 10.1016/j.applthermaleng.2011.04.040
- Promvong, P. and S. Kwankaomeng, 2010. Periodic laminar flow and heat transfer in a channel with 45° staggered V-baffles. Int. Commun. Heat Mass Transfer, 37: 841-849. DOI: 10.1016/j.icheatmasstransfer.2010.04.002
- Promvong, P., S. Skullong, S. Kwankaomeng and C. Thiangpong, 2012a. Heat transfer in square duct fitted diagonally with angle-finned tape-Part 2: Numerical study. Int. Commun. Heat Mass Transfer, 39: 625-633. DOI: 10.1016/j.icheatmasstransfer.2012.03.010
- Promvong, P., S. Sripattanapipat and S. Kwankaomeng, 2010a. Laminar periodic flow and heat transfer in square channel with 45° inline baffles on two opposite walls. Int. J. Thermal Sci., 49: 963-975. DOI: 10.1016/j.ijthermalsci.2010.01.005
- Promvong, P., W. Jedsadaratanachai and S. Kwankaomeng, 2010b. Numerical study of laminar flow and heat transfer in square channel with 30° inline angled baffle turbulators. Applied Thermal Eng., 30: 1292-1303. DOI: 10.1016/j.applthermaleng.2010.02.014
- Promvong, P., W. Jedsadaratanachai, S. Kwankaomeng and C. Thiangpong, 2012b. 3D simulation of laminar flow and heat transfer in V-baffled square channel. Int. Commun. Heat Mass Transfer, 39: 85-93. DOI: 10.1016/j.icheatmasstransfer.2011.09.004
- Sriromreun, P., C. Thiangpong, P. Promvong, 2012. Experimental and numerical study on heat transfer enhancement in a channel with Z-shaped baffles. Int. Commun. Heat Mass Transfer, 39: 945-952. DOI: 10.1016/j.icheatmasstransfer.2012.05.016
- Versteeg, H.K. and W. Malalasekera, 2007. An Introduction to Computation Fluid Dynamics. 2nd Edn., Pearson Education, ISBN-10: 9780131274983.